The effect of work-hardening and pile-up on nanoindentation measurements

J. D. Gale · A. Achuthan

Abstract Nanoindentation is performed on the cross-section of copper samples subjected to surface mechanical attrition treatment (SMAT). The cross-section of the SMAT samples provides a unique microstructure with varying amounts of work-hardening depending on the distance from the SMAT surface. Results show that for a given indentation load the pile-up height decreases and the indentation depth increases as the distance from the SMAT surface increases, both following a power law relationship. Based on image analysis of the indented surface this increase in the pile-up height and decrease in indentation depth is attributed to the localization of plastic strain due to the increased resistance to dislocation motion in the work-hardened region. For a given amount of work-hardening (in terms of distance from SMAT surface), the indentation depth increased with the indentation load obeying a power law relationship with the exponent ranging from 0.58 to 0.68. However, the pile-up height increased linearly with the load, with the rate (slope) increasing with the amount of work-hardening. The observed linear increase in pile-up height with indentation load would naturally introduce an indentation size effect (ISE) if the hardness is corrected for the pile-up. Interestingly, this ISE associated with pile-up increased with an increase in indentation depth, in contradiction to the ISE associated with strain gradient. Deviation of the hardness values corrected for pile-up from the bulk behavior due to surface effect is highlighted and a method to obtain a bulk-equivalent hardness quantity representing the bulk behavior is proposed.

J. D. Gale · A. Achuthan (✉)
Department of Mechanical & Aeronautical Engineering,
Clarkson University, Potsdam, NY 13699, USA
e-mail: aachutha@clarkson.edu

Introduction

Nanoindentation is an excellent method for characterizing material properties of both bulk- and thin-film materials. Mechanical properties such as modulus, indentation hardness, yield strength, elastic work, and plastic work associated with nanoscale deformation can be obtained from the indentation load–depth curve [1–3]. However, nanoindentation measurements are often prone to errors from various sources. The impact of these errors is expected to be more prominent for low load indentation experiments, which are often used to investigate various nanoscale deformation phenomena such as indentation size effect (ISE) [4] and displacement bursts [5]. Material properties or the deformation phenomena of interest in most of these measurements is associated with the bulk material, meaning any deviation of the surface deformation from the bulk, contributes to errors in the measurement. Residual deformation from mechanical polishing on the surface [6, 7] and pile-up/sink-in of the material around the indenter-tip [8] are two such surface effects that could lead to significant error in the determination of material properties. The pile-up/sink-in phenomenon observed in various materials during nanoindentation causes significant underestimation of the projected contact area of the indent determined using the tip area function method [9]. Underestimation of the true contact area by as much as 60 % has been reported to occur in these measurements depending on the severity of the pile-up [8]. Correlating pile-up to various material and loading conditions by experimental characterization can be invaluable in accounting for the effect of pile-up appropriately on hardness and other nanoscale deformation mechanisms [10].

Pile-up height has been shown to vary with the indentation load and the work-hardened condition of the

material. This makes accounting for pile-up correction in the determination of hardness a difficult task [11]. Many studies have shown that the formation of pile-up/sink-in can be correlated to the elastic and plastic regimes of deformation through various parameters such as elastic strain at yield (σ_y/E), the ratio of the final indentation depth to maximum indentation depth (h_f/h_{max}), and the strain hardening exponent (n) [8, 11–15]. A material with a larger elastic strain at yield (i.e., smaller σ_y/E) and smaller n was found to exhibit a larger amount of pile-up when compared to a material with a lower elastic strain at yield and a higher value of n [8]. However, accurately determining σ_y and n from the indentation load-depth behavior is a very difficult task, especially when the response is already influenced by pile-up formation. Therefore, an experimentally measured ratio between h_f and h_{max} is commonly used to determine the prevalence of pile-up. It is suggested that a material with a low ability to work harden and a numerical value greater than 0.7 for the ratio h_f/h_{max} will exhibit pile-up. However, as presented in this study, the ratio h_f/h_{max} does not capture the effect of work-hardening on pile-up formation.

Previous studies, primarily driven by the intention to correlate the variation in pile-up height to bulk mechanical properties, contributed significantly in demonstrating the role of elastic and plastic regimes of deformation on pile-up formation. Correlating pile-up to bulk mechanical properties is an important step in quantifying its effect and accounting for its role on indentation measurements. However, such an approach requires extensive experimental verification since the deformation at a small scale may involve various mechanisms, all of which contribute to size effects that cannot be captured by standard continuum models. Interestingly, most of the theoretical development reported were based on finite element modeling studies, validated with limited experimental data.

The limited experimental studies reported in literature are based on investigating either annealed samples or highly work-hardened samples [10, 16–18], demonstrating increased pile-up formation in work-hardened samples. In McElhaneys work [16], the annealed single crystal copper sample was found to have very little pile-up when compared to work-hardened polycrystalline copper sample. Development of an empirical relationship for estimating the pile-up contact area by determining the pile-up contact area for several peak indentation loads using atomic force microscopy has also been reported [10]. The average pile-up lobe-width a_{av} (or lobe-height) was found to vary linearly with the indentation load during Berkovich indentation using loads of 25 to 200 mN [10]. On the contrary, it was demonstrated that a power fit of the form, $a_{av} = AP^n$, had a better correlation based on pile-up measurement on

annealed Cu and Cu-H58 copper samples [18]. The n value was 0.24 and 0.38 for work-hardened and annealed samples, respectively. Accounting for pile-up using the plastic work and plastic deformation volume has also been suggested [19]. Investigating only the two extreme sample conditions in these experimental studies, i.e., fully annealed and highly work-hardened, although providing some insight into the mechanism of pile-up formation, limits our ability to understand the dependence of dislocation density on pile-up formation. In addition, the pile-up formation has the potential to introduce inhomogeneous deformation at a small scale that could lead to size dependent properties [10, 18].

Corrections to the standard Oliver and Pharr method [9] have previously been proposed as a method to account for errors in hardness measurement due to pile-up formation. There are three direct methods reported in literature, two of which rely on SPM/AFM imaging of the indent, referred to as the Lobe and Geometry methods, and the third referred to as the Corner's method [18]. Since the material surface is raised due to pile-up, the imaging-based hardness corrections for pile-up (or sink-in) phenomena are based on the consideration that the contact area determined from the tip-area function is smaller (or larger for sink-in) than that corresponding to the raised surface. Hence, this under-predicted tip-area is corrected by adding the difference in the area estimated by various methods for pile-up (subtracting for sink-in) [3, 10, 16, 18, 20–22].

An alternative to the direct method discussed above is a method based on the work of indentation, determined as the area under the load-depth curve during indentation [2, 23–25]. The work of indentation method calculates hardness by taking the total area under the resulting indentation curve (total work of indentation), or by the plastic work performed during indentation (plastic work of indentation). This method is more straight forward when compared to the SPM/AFM methods and leaves less calculation to the discretion of the observer; however, its accuracy is highly debatable [18].

This work presents a study on the effect of pile-up on hardness measurements, investigated by indenting on the cross-section of copper samples subjected to surface mechanical attrition treatment (SMAT). The cross-section of a SMAT sample exposes a surface with the degree of work-hardening varying continuously; an ideal sample for studying the effect of work-hardening on pile-up formation and other low load deformation phenomena. Variations in pile-up height, indentation depth, and the nature of surface deformation on this surface was studied. The results demonstrated that the effect of pile-up on hardness is significantly higher for high-load indentation, rather than low-

load indentation as expected. For a given location from the SMAT face, the pile-up height increased linearly with the indentation load, introducing size dependence in hardness measurements. Hardness correction for pile-up, considering this linear variation, is derived. It is shown that the hardness values corrected for pile-up following the conventional approach will deviate from the bulk deformation behavior due to the surface effect. Accordingly, an equivalent hardness measurement capturing the bulk material deformation is derived.

Experiments

SMAT specimen preparation

Bar stock of 25.4 mm diameter copper alloy 101 (99.99 % Cu) was used in this study. The bar was cut into 12-mm thick disks, mechanically polished, and then annealed in a vacuum furnace at 700 °C for 1 h. Coarse polishing was accomplished using a sequence of 320, 600, 800, and 1200 grit silicon carbide paper. After coarse polishing, specimens were diamond polished with 3 and 1 μm Buehler Meta-Di-diamond suspension. Annealing removed the mechanical deformation effects of polishing. The grain size of the annealed specimens was estimated to be mostly in the range of 40–100 μm.

Annealed specimens were subjected to SMAT for 15 min. The SMAT process was accomplished by using a dome shaped vacuum sealed refractory chamber attached to a Labworks Inc. LW-139-40 Electrodynamic Shaker System. The chamber was vibrated at a resonant frequency of 31 Hz, with the specimen clamped to the top of the dome refractory chamber and subjected to the impact of ten 6 mm tungsten carbide spheres. Further details on the SMAT process have been documented in a previous article [7].

After SMAT, the specimens were cross sectioned using a Buehler Isomet low speed saw. Each cross section was then mounted in an epoxy resin and mechanically polished. The mechanical polishing was followed by 900 min of electrochemical polishing in Ortho-phosphoric acid to remove any residual mechanical deformation induced by mechanical polishing. A careful analysis of the impact of polishing on the surface was first conducted to identify the ideal electrochemical polishing conditions necessary to remove all the residual polishing effect from the surface [7]. This was critical to confirm that for a given maximum indentation load, the variability in pile-up height is solely due to the variability in work-hardening of the sample. The surface was extensively tested to confirm the complete removal of residual deformation from mechanical polishing [7].

Indentation testing

Nanoindentation was performed using a Hysitron TI-950 Triboindenter with a 100 nm radius Berkovich tip along the depth of the cross-section. Prior to indentation testing calibration of the transducer and optics was performed. A tip-area calibration was also performed on a standard quartz sample for tip radius verification. Various load controlled indentations under maximum loads of 1, 2, 3, and 5 mN were conducted. After indentation, each indent was SPM imaged using the same Berkovich tip. The pile-up height and indentation depth corresponding to a given maximum load at a given location reported in this study are based on three indentation tests, two on one sample, and a third on a second sample. Average results are reported with error bars indicating standard deviation.

The indent profiles were taken by performing three line scans across the sample surface, on a straight line that intersects the largest pile-up location for each indent. The largest pile-up height on an edge is determined by running a line scan along a pile-up ridge and the vertex opposite to that ridge. Pile-up formation was not exactly symmetric; therefore, an average value of the largest heights measured from each of the three edges of an indent was used as the pile-up height for that indent [20].

Results

A schematic of the SMAT sample cross-section, illustrating the expected variation in the work-hardening and the dislocation density is shown in Fig. 1. The amount of work-hardening and the dislocation density decreases continuously throughout the thickness of the sample as the distance from the SMAT surface increases.

Post-nanoindentation SPM imaging using a Berkovich tip showed a large difference in the surface deformation characteristics between an annealed copper sample and a work hardened SMAT-15 sample near the SMAT surface (Fig. 2). Indentation on the annealed copper with a load of 5 mN showed relatively smaller pile-up (<20 nm) when compared to that at location 400 μm from the SMAT
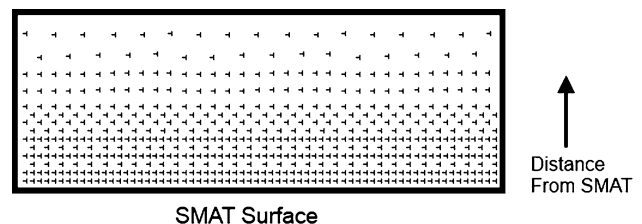

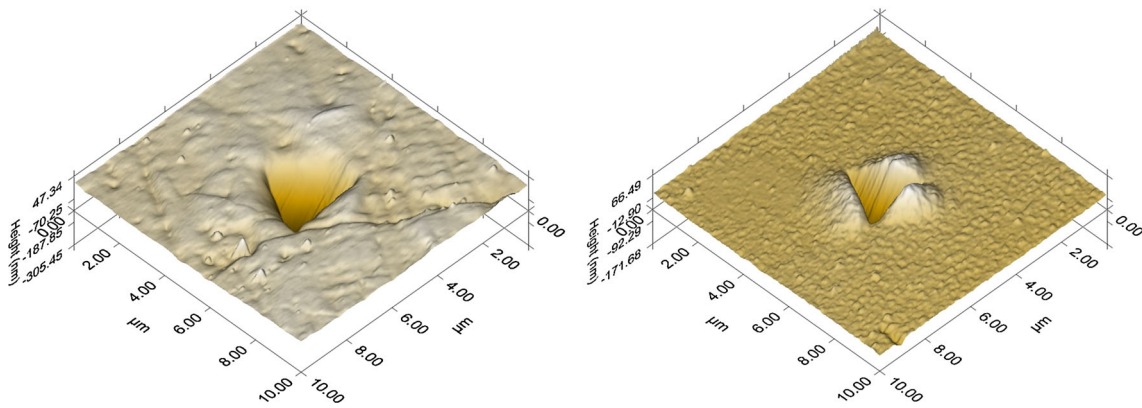**Fig. 1** Schematic representing the variation in work-hardening along the thickness of a SMAT sample

Fig. 2 SPM images of annealed and SMAT-15 Copper after indentation with a load of 5 mN, showing the change in pile-up after severe work-hardening

Fig. 3 Pile-up height versus distance from the SMAT surface for various maximum indentation loads (**a**), indentation depth versus distance from the SMAT surface for various maximum indentation loads (**b**)
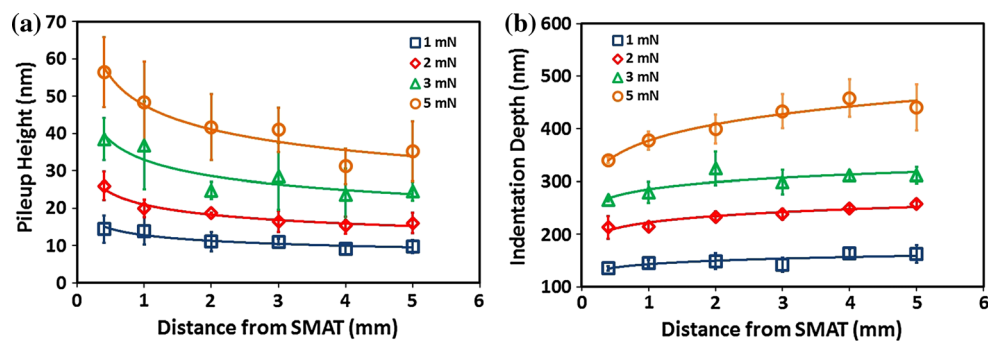
surface (55 nm) (Fig. 2). In addition, the pile-up formation was more localized with well defined features in the work hardened sample compared to that of the annealed sample.

Significant variation in pile-up height and indentation depth was found between indents performed close to the SMAT surface when compared to those performed farther away. This variation in pile-up height and indentation depth compared against the distance from the SMAT surface is shown in Fig. 3a, b, respectively. A power law data fit with appropriate values for the power n was considered for the pile-up height and the indentation depth variation, which showed satisfactory agreement (Fig. 3a). As the distance from the SMAT surface increased, i.e., the work-hardening and dislocation density decreased, the pile-up height decreased and the indentation depth increased as expected. It is important to note that the sensitivity of pile-up height and indentation depth with respect to the distance from the SMAT surface, both increased with an increase in indentation load. The depth of the work-hardened zone in terms of the variation in pile-up height and indentation depth is approximately 2–5 mm from the SMAT surface, depending on the maximum indentation load. This depth of the work-hardened zone is the same as that determined based on hardness measurements (without consideration of pile-up) reported in a previous study [7].

The pile-up height and indentation depth are plotted against the indentation load in Fig. 4a, b, respectively. Interestingly, the variation in pile-up height plotted against maximum indentation load at a given distance from the SMAT surface did not follow a $\sqrt{P}$ behavior, with P being indentation load, as expected under self-symmetric conditions (Fig. 4). Instead a strong linear relationship with a regression coefficient above 99 % was observed for all cases. The sensitivity of the pile-up height relationship with regard to indentation load, represented by the slope in Fig. 4a, in general increased with an increase in work-hardening. Contrary to the linear increase in pile-up height with an increase in maximum indentation load, the indentation depth behavior still matched reasonably well to a $\sqrt{P}$ relationship (Fig. 4b). Curve fitting of the data with a power law relationship yielded a good agreement with a regression coefficient of 97 % and above, for the exponent n ranging between 0.58 to 0.69 depending on the degree of work-hardening. As the work-hardening increased the behavior favored more and more toward the $\sqrt{P}$ relationship.

Figure 5 shows the variation of surface deformation with an increase in the distance from the SMAT surface obtained for a 5 mN load indentation. Pile-up expanded

Fig. 4 Pile-up height versus indentation load for various locations in the SMAT region (**a**), and indentation depth versus indentation load for various locations in the SMAT region (**b**)
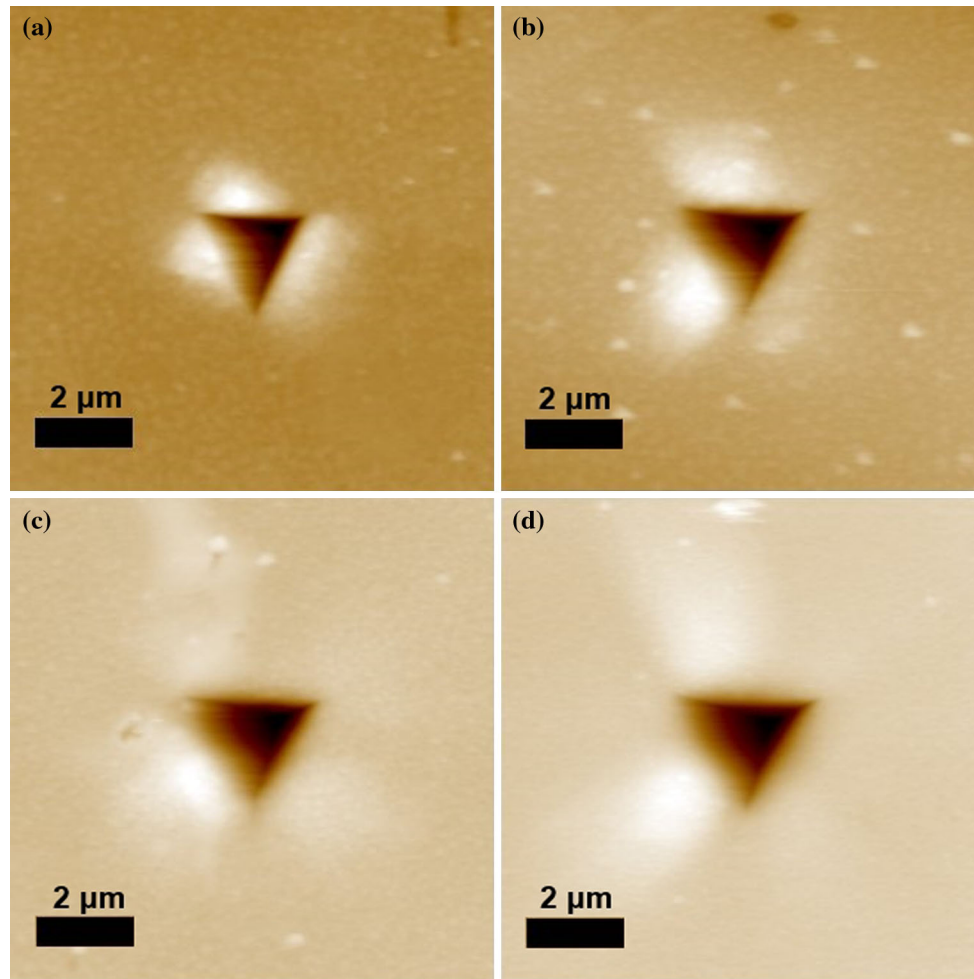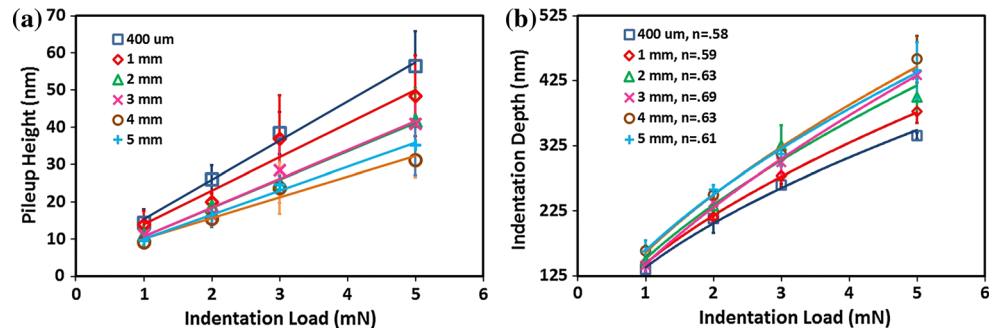

Fig. 5 SPM images of indents performed across the cross-section of a SMAT-15 copper sample under 5 *mN* load shows that the deformation is confined more and more with an increase in work-hardening.

Images taken at a distance of 200 μm (**a**), 2 mm (**b**), 5 mm (**c**), and 10 mm (**d**), from the SMAT-15 treated surface

outward and its height decreased as the indentation location moved farther away from the SMAT edge. For example, at 5 mm from the SMAT edge, the white pile-up region is clearly more widespread and not confined to the edges of the indenter (Fig. 5c), compared with the pile-up region at 400 μm (Fig. 5a) and 2 mm (Fig. 5b). A continued gradual variation of this behavior was observed in the SMAT zone,

though only four locations are shown here. The observed behavior clearly demonstrates that the deformation is confined more locally in the vicinity of the indenter tip with an increase in the amount of work-hardening.

The surface deformation at 400 μm from the SMAT surface, corresponding to four different indentation loads is shown in Fig. 6. The plastic deformation region near the
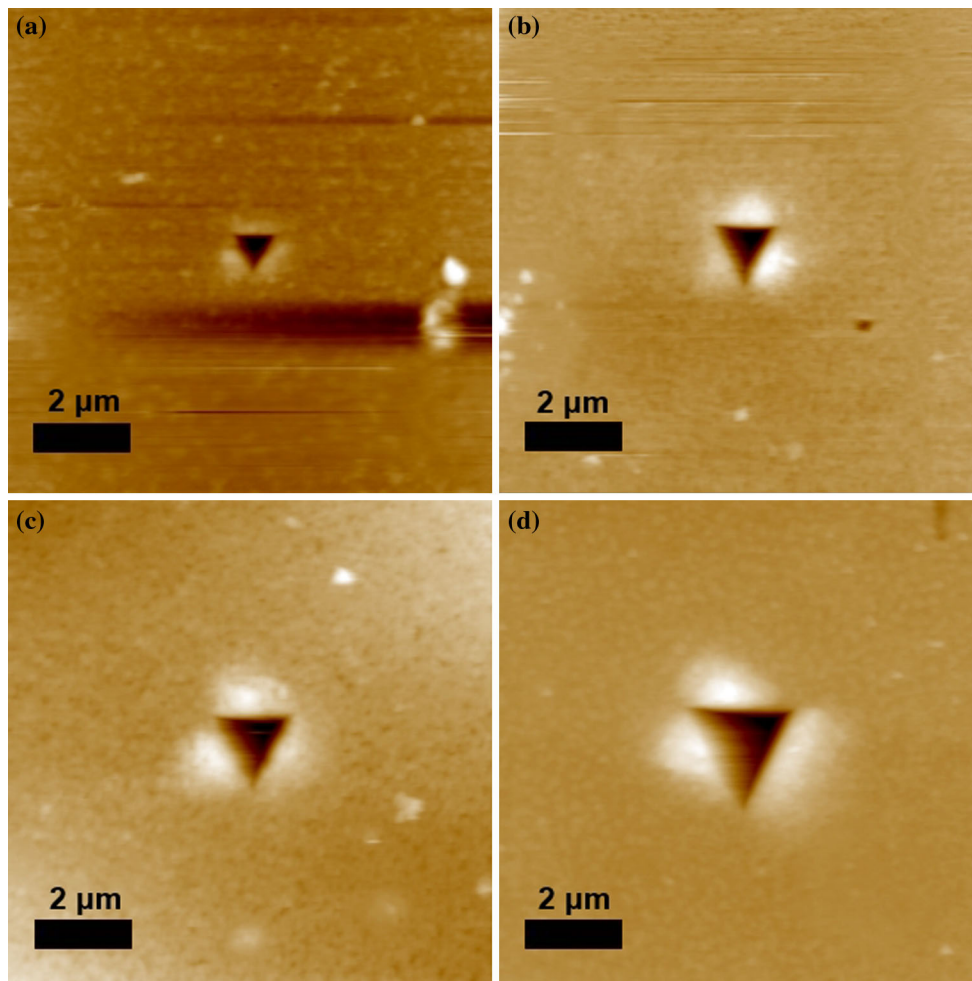
Fig. 6 SPM images of indents performed on the cross-section of a SMAT-15 copper sample 400 μm away from the SMAT edge. Images taken after indentation loads of 1 mN (**a**), 2 mN (**b**), 3 mN (**c**), and 5 mN (**d**)

indenter tip increased in size with an increase in the indentation load, which can be seen when comparing Fig. 6a for a 1 mN indentation load, all the way to Fig. 6d for a 5 mN indentation load. However, when compared to the variation in the nature of deformation with work-hardening (Fig. 5), the nature of deformation remained the same in this case, differing only in the size of deformation.

Discussion

Mechanism of pile-up formation

From the observed increase in local confinement of the surface deformation (increase in pile-up height and decrease in indentation depth as the distance from the SMAT surface increases), the present study offers a solid experimental proof that the higher resistance to dislocation motion is the fundamental mechanism driving pile-up

formation in work-hardened samples. This mechanism can be explained as follows. During indentation, when the elastic energy density in a material around the indenter-tip reaches a critical value incipient plasticity driven by dislocation motion ensues. A further increase in deformation from an increase in load, will have both elastic and plastic contributions. Depending on the material and its microstructural conditions, the plastic deformation due to dislocation motion could be accommodated into the bulk volume without causing any significant surface deformation. However, for a material with a large dislocation density as in work-hardened metal, there is significant resistance to dislocation motion. Hence, the elastic deformation and the associated elastic energy density will be relatively larger in the material around the indenter-tip. Larger elastic energy density around the indenter-tip in the presence of an increased resistance from the bulk drives the deformation to the free surface. In other words, the resistance to dislocation motion due to a larger dislocation

density not only confines the plastic zone as the work-hardening increases (Fig. 5), but also forces the material to deform more toward the surface rather than fully deforming into the volume (Fig. 3).

Based on finite element simulations under a wide range of sample conditions in terms of strain hardening coefficient n and E/σ_y ratio, the pile-up formation in work-hardened material has been hypothesized as the result of the combined effect of localization of plastic strain and the decrease in total plastic deformation [26]. The decrease in the strain hardening coefficient n due to work-hardening is a measure of the decrease in material's ability to further work-harden. As the ability to work-harden decreases with an increase in work-hardening, the uniaxial stress–strain behavior of bulk material tends more and more towards perfect plastic behavior, which explains the localization of plastic deformation around the indenter-tip. The decrease in the E/σ_y ratio with an increase in work-hardening, in general, is a measure of the decrease in total plastic deformation and the associated increase in elastic strain energy density. The results from the present study, agree in principle, with the correlation of pile-up height with the E/σ_y ratio and the strain hardening coefficient n, derived using finite element simulations [8]. However, a direct correlation of the strain hardening coefficient n and the E/σ_y ratio to the characteristics of nanoindentation load-depth behavior is quite challenging. Moreover, the individual effects of the localization of plastic strain and the decrease in total plasticity on the mechanism of pile-up formation is still not well understood (localization of plastic deformation does not necessarily produce pile-up formation if the material still has the ability to accommodate the resulting local plastic deformation into the bulk volume).

Correlating pile-up formation with the characteristics of indentation load-depth behavior, if possible, would be quite valuable in accounting for the error due to pile-up formation in hardness measurement. Most of the studies reported in literature derived such correlations by simulating nano-indentation using finite element models. The h_f/h_{max} ratio, a parameter that is widely recommended as a promising quantity to capture the pile-up height variation along with the strain-hardening coefficient n, is quite attractive since it can be determined very easily from nanoindentation tests [8]. Based on finite element studies, it is suggested that a value of 0.7 and above for h_f/h_{max} in work-hardened samples will lead to pile-up and any value below 0.7 will result in sink-in. The h_f/h_{max} ratio obtained for various cases in the present study is shown in Fig. 7. With the h_f/h_{max} ratio being well above 0.7 for all the various cases of work-hardening, the results from the present study agree with the conclusions drawn from the finite element studies. However, it is important to note that the h_f/h_{max} remains
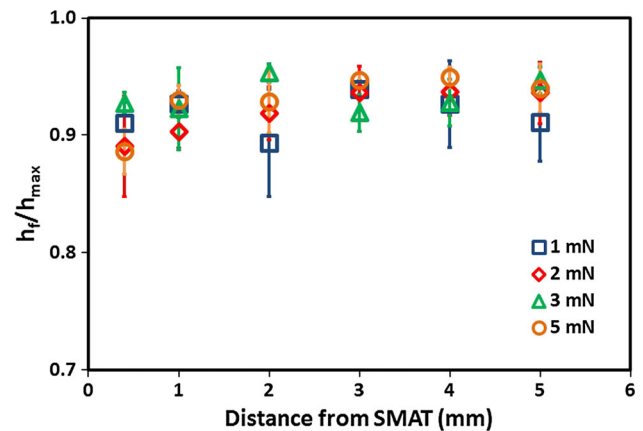

Fig. 7 Variation of h_f/h_{max} ratio with distance from the SMAT surface

the same for all these cases even when there was significant variation in pile-up height depending on the indentation load and work-hardening conditions. Pileup at the SMAT edge was very large compared with the pile-up at the far edge of the sample, but h_f/h_{max} variation was insignificant, mostly in the range of 0.9–0.95. Hence, it can be concluded from the experimental results that the h_f/h_{max} ratio, though useful to determine whether the indentation will result in pile-up or sink-in, is not a useful parameter for quantitatively correlating pile-up characteristics.

Indentation size effect (ISE)

As shown in Fig. 6 for a given location closer to the SMAT surface, the nature of surface deformation remained the same with an increase in load, changing only in its size, for all the locations irrespective of the distance from the SMAT surface. This qualitative observation of the surface deformation scaling with the indentation load, in addition to the linear variation of pile-up height and the power law relationship of the indentation depth with indentation load indicates that the deformation merely scales with the load. However, the linear variation of pile-up height with the indentation load for any given dislocation density is quite remarkable with major consequences in hardness measurements, especially when the indentation depth followed closer to the $\sqrt{P}$ behavior expected in self-symmetric indentation (Fig. 4). The linear behavior of pile-up height with indentation load determined in the present study is consistent with the experimental study reported previously, where the pile-up lobe width was found to vary linearly in the case of a soda-lime sample [10]. In the case of annealed and work-hardened copper also, the pile-up lobe height did not follow a $\sqrt{P}$ relationship with the load [18].

A major consequence of the linear behavior of pile-up height is that its contribution to the contact area projected

to the top of the pile-up formation varies quadratically, thereby introducing ISE. The sensitivity coefficient n for the indentation depth to indentation load relationship with values larger than 0.5 and the overall decrease in n with an increase in work-hardening are indicative of ISE associated with a strain gradient. The plastic strain gradient being inversely proportional to indentation depth, as the indentation depth decreases the strain gradient increases along with the associated geometrically necessary dislocations (GND's) leading to ISE. However, since the ISE associated with the linearity of pile-up height with indentation load increased with an increase in the indentation load, it cannot be explained based on the plastic strain gradient ($1/h$) theory. This is also evident from the fact that the observed linear behavior was more sensitive as the work-hardening increased, while the ISE resulting from a strain gradient is expected to be relatively weaker due to a larger amount of statistically stored dislocations (SSDs).

Under spherical indentation, the indentation depth variation with indentation load has a characteristic behavior closer to linearity in the low indentation load regime. However, the possibility of the rounding-off of the Berkovich indenter-tip as the mechanism for the observed linear behavior of pile-up height has been discarded in the present study due to the following two reasons; (1) a relatively new indenter-tip was used in the present study and all the recommended calibrations were thoroughly followed, and (2) the pile-up deformation volume being relatively farther away from the indenter tip, the rounding off would have resulted in a linear relationship for the indentation depth before it could introduce a linear relationship for the pile-up formation.

The increase in the sensitivity of the relationship between pile-up height and indentation load, and the decrease in the sensitivity of the relationship between indentation depth and indentation load, with an increase in work-hardening, as shown in Fig. 3, is a measure of resistance to plastic deformation of the bulk material. Due to the larger resistance to dislocation motion with an increase in work-hardening, the part of the volume that deforms toward the surface increases, while the part of the deformation volume that deforms into the bulk decreases. This is quite evident in the plot showing the ratio of pile-up height to indentation depth (Fig. 8). As the work-hardening increased, the ratio of pile-up height to indentation depth increased significantly with an increase in the indentation load. This increase in the sensitivity of the pile-up ratio with an increase in the degree of dislocation density has a very interesting consequence. Contrary to the expected decrease in error associated with surface effects as the deformation volume increases, the observed higher sensitivity shows that the impact of pile-up is higher as the indentation depth increases in samples subjected to a larger amount of work-hardening.
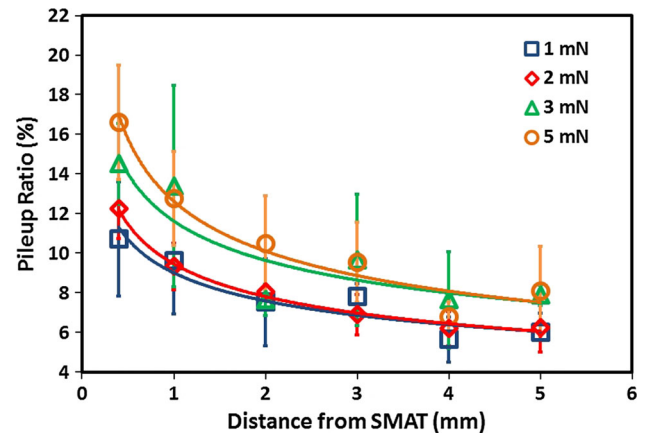

Fig. 8 Pile-up height to indentation depth ratio versus distance from the SMAT surface for various maximum indentation loads

Hardness correction for pile-up

Since the contact surface is raised due to pile-up, most hardness corrections for the pile-up phenomena are based on the consideration that the contact area determined from the tip-area function is smaller than that corresponding to the raised surface [3, 10, 16, 18, 20–22]. Hence, this underestimated tip-area is corrected by adding the difference in the area estimated by using the corrected indentation depth. The corrected indentation depth can be obtained as below (Fig. 9a),

$$hc = hc_{OP} + h_{pu}. \tag{1}$$

Considering the linear variation of pile-up height with indentation load (P) the above relationship can be written as,

$$hc = hc_{OP} + \kappa(\rho_s)P, \tag{2}$$

where $\kappa(\rho_s) = \frac{\Delta h_{pu}}{\Delta P}$ is the slope of pile-up height to indentation load relationship which is a function of work-hardening (or statistically stored dislocation density, ρ_s). Hence, by determining the slope using a single measurement of pile-up height for a given indentation load the corrected indentation depth can be obtained for any other indentation loads using the above relationship (the small y-intercept in the relationship is ignored, Fig. 4a).

It is important to note that the corrected hardness does not accurately reflect the behavior of the bulk material due to the effect of surface deformation in the form of pile-up formation. The lack of a free surface in the bulk means a deformation equivalent to the pile-up formation, where the material deforms to the surface as a response to the stress is not viable in the bulk. Hence, an equivalent hardness measurement that reflects the bulk material property should be larger, not smaller, than the one determined based on the Oliver–Pharr method. This discrepancy can be addressed

Fig. 9 Schematic showing conventional correction method (**a**) and bulk-equivalent hardness method (**b**)
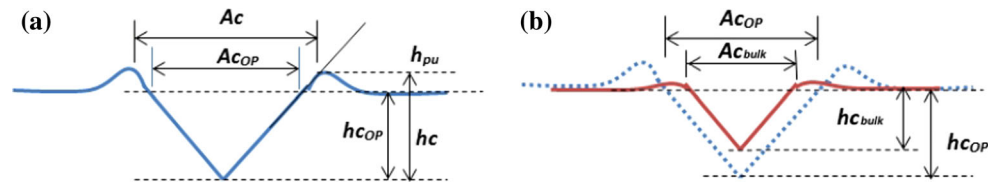
either by accounting for the surface effect on the bulk material properties after these properties are derived from the hardness measurement corrected for the pile-up, or by deriving a bulk-equivalent hardness that reflects the bulk property from which the bulk properties can be derived. The bulk-equivalent hardness can be derived in terms of an equivalent indentation depth (hc_{bulk}) as discussed below.

The deformation in the bulk can be visualized by considering a scenario where the piled up material is pushed back into the bulk material to level the surface using an external load, while the indenter is still exerting the maximum load. This external load can be considered as the resistance from the bulk material in the absence of a free surface. To accommodate the deformation due to the pushing back of the pile-up the indenter has to rise upward (Fig. 9b). The resulting hc_{bulk} and Ac_{bulk} shown in Fig. 9b corresponds to the bulk-equivalent hardness, reflecting the bulk material behavior.

The corrected indentation depth corresponding to bulk-equivalent hardness that reflects bulk material behavior can be obtained as,

$$hc_{bulk} = hc_{OP} - f_V h_{pu}, \qquad (3)$$

where hc_{OP} is the effective contact depth calculated using the Oliver and Pharr method, and hc_{bulk} is the effective contact depth corresponding to the bulk-equivalent hardness. The f_V is a factor that is a measure of the amount of pile-up volume that would have been accommodated by the bulk deformation volume under the indenter in the absence of the free surface.

Considering the observed linear variation in pile-up height with indentation load,

$$hc_{bulk} = hc_{OP} - f_V \kappa(\rho_s) P. \qquad (4)$$

Hardness determined from indentation data on the SMAT surface based on six different methods and the proposed method (for a f_V value of unity) are shown in Fig. 10 for a 3 mN indentation load. These methods include the standard Oliver and Pharr method [9], where the indenter-tip profile information is used to determine the indent area and the work of indentation (both total and plastic work) computed using standard analytic formulation [2, 18, 23]. In addition, the hardness was also determined using the work of indentation approach measured numerically from a quadratic fit of the resulting load–depth data. Interestingly, the values of total work and plastic work of indentation found
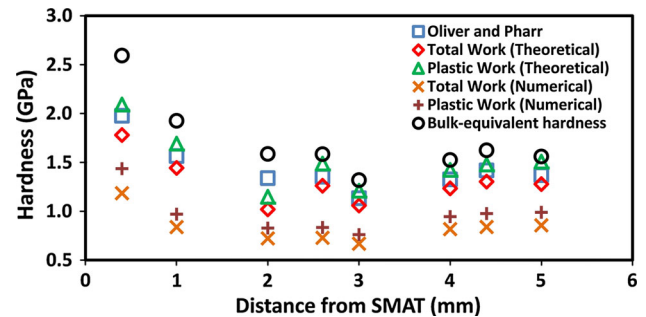

Fig. 10 Nanoindentation hardness calculated using various techniques

by using numerical integration on indentation curves from SMAT-treated samples do not match those calculated using analytical methods. The hardness values obtained using the work of indentation method determined numerically was much smaller than that determined by the Oliver and Pharr method and the theoretically calculated work of indentation [19]. The bulk-equivalent hardness as expected, predicted the highest values for hardness.

Conclusion

In this study, pile-up height during nanoindentation of a SMAT copper cross-section was analyzed using SPM imaging. As the amount of work-hardening increased, the plastic zone became more and more confined locally, due to the resistance to dislocation motion in the bulk. The localization of the plastic zone with an increase in work-hardening resulted in larger pile-up height and smaller indentation depth. Pile-up and indentation depth showed a power law relationship with the distance from the SMAT surface.

Correlation of pile-up formation with material properties as hypothesized by previous studies using finite element modeling was verified. Contrary to the finite element model prediction, the results from the present study demonstrated that the h_f/h_{max} ratio does not accurately capture the effect of work-hardening on pile-up formation.

The increase in pile-up height, indentation depth, and surface deformation with an increase in indentation load was due to the deformation scaling with the load. Pile-up height showed a strong linear correlation with the indentation load, while indentation depth followed a power law

relationship with the exponent ranging between 0.58 and 0.69. The rate at which pile-up height and indentation depth increased with the indentation load was a function of the amount of work-hardening. This rate increased with an increase in work-hardening for pile-up height, while it decreased for indentation depth. A major consequence of the linear behavior of pile-up height variation with indentation load was the resulting ISE in hardness measurement. Contradictory to the ISE associated with a strain gradient, the ISE associated with pile-up formation increases with an increase in the amount of work-hardening.

Based on the bulk volume deformation consideration, it is demonstrated that the conventional correction method for calculating projected contact area will result in the hardness properties deviating substantially from the bulk material behavior. Therefore, a bulk-equivalent hardness property that reflects the bulk behavior is derived. This bulk-equivalent hardness value can be used to approximate hardness values in the event that pile-up is evident in the material.

References

1. Lucca DA, Herrmann K, Klopfstein MJ (2010) Nanoindentation: measuring methods and applications. CIRP Ann Manuf Technol 59(2):803–819
2. Ma D, Ong CW (2010) Analytical relationship among nominal hardness, reduced Young's modulus, the work of indentation, and strain hardening exponent. J Mater Sci 45(9):2530–2533. doi:10.1007/s10853-010-4289-7
3. Zhu L, Xu B (2010) Measurement of residual stress in quenched 1045 steel by the nanoindentation method. Mater Charact 61(12):1359–1362
4. Nix WD, Gao H (1998) Indentation size effects in crystalline materials: a law for strain gradient plasticity. J Mech Phys Solids 46(3):411–425
5. Shim S, Bei H, George EP, Pharr GM (2008) A different type of indentation size effect. Scripta Mater 59(10):1095–1098
6. Wang Z, Bei H, George EP, Pharr GM (2011) Influences of surface preparation on nanoindentation pop-in in single-crystal mo. Scripta Mater 65(6):469–472
7. Gale J, Achuthan A, Morrison D (2013) Indentation size effect (ISE) in copper subjected to severe plastic deformation (SPD). Metall Mater Trans A. doi: 10.1007/s11661-014-2201-9
8. Bolshakov A, Pharr GM (1998) Influences of pileup on the measurement of mechanical properties by load and depth sensing indentation techniques. J Mater Res 13(4):1049–1058
9. Oliver WC, Pharr GM (1992) Improved technique for determining hardness and elastic modulus using load and displacement sensing indentation experiments. J Mater Res 7(6):1564–1580
10. Kese K, Li ZC (2006) Semi-ellipse method for accounting for the pile-up contact area during nanoindentation with the Berkovich indenter. Scripta Mater 55(8):699–702
11. Taljat B, Pharr GM (2004) Development of pile-up during spherical indentation of elastic plastic solids. Int J Solids Struct 41(14):3891–3904
12. Wang J, Hodgson PD, Yang C (2012) Effects of mechanical properties on the contact profile in Berkovich nanoindentation of elastoplastic materials. J Mater Res 27(1):313–319
13. Rodriguez J, Garrido Maneiro MA (2007) A procedure to prevent pile up effects on the analysis of spherical indentation data in elasticplastic materials. Mech Mater 39(11):987–997
14. Cheng Y-T, Cheng C-M (1998) Effects of 'sinking in' and 'piling up' on estimating the contact area under load in indentation. Philos Mag Lett 78(2):115–120
15. Cheng Y-T, Cheng C-M (2000) What is indentation hardness? Surf Coat Technol 133–134:417–424
16. McElhaney KW, Vlasssak JJ, Nix WD (1998) Determination of indenter tip geometry and indentation contact area for depth-sensing indentation experiments. J Mater Res 13:1300–1306
17. Wang Y, Raabe D, Klber C, Roters F (2004) Orientation dependence of nanoindentation pile-up patterns and of nanoindentation microtextures in copper single crystals. Acta Mater 52(8):2229–2238
18. Cabibbo M, Ricci P (2013) True hardness evaluation of bulk metallic materials in the presence of pile up: analytical and enhanced lobes method approaches. Metall Mater Trans A 44(1):531–543
19. Zhou L, Yao Y (2007) Single crystal bulk material micro/nano indentation hardness testing by nanoindentation instrument and AFM. Mater Sci Eng A 460461:95–100
20. Lee Y-H, Baek U, Kim Y II, Nahm S-H (2007) On the measurement of pile-up corrected hardness based on the early Hertzian loading analysis. Mater Lett 61(19–20):4039–4042
21. Zhu L, Xu B (2012) Effect of residual stress on the nanoindentation response of (100) copper single crystal. Mater Chem Phys 136:561–565
22. Lee J-M, Lee C-J, Lee K-H, Kim B-M (2012) Effects of elastic–plastic properties of materials on residual indentation impressions in nano-indentation using sharp indenter. Trans Nonferr Metal Soc China 22(Supplement 3):s585–s595
23. Tuck JR, Korsunskyl AM, Bull SJ, Davidson RI (2001) On the application of the work-of-indentation approach to depth-sensing indentation experiments in coated systems. Surf Coat Technol 137(2–3):217–224
24. Zhao X, Wang F, Hang J, Liu T (2012) Determining the mechanical properties of solid oxide fuel cell by an improved work of indentation approach. J Power Sources 201:231–235
25. Guclu N, Kolemen U, Uzun O, Celebi S (2005) Work of indentation approach for investigation of mechanical properties of YBCO bulk superconductor at cryogenic temperatures. Physica C 433:115–122
26. Barnoush A (2012) Correlation between dislocation density and nanomechanical response during nanoindentation. Acta Mater 60(3):1268–1277